Physical Chemistry 2022, 11(1): 1-10
DOI: 10.5923/j.pc.20221101.01

Protective Action of Air in the Dissolution of Aluminium in Acid Solutions Containing Chloride Ions at Room Temperature

B. A. Abd-El-Nabey[1], S. El-Housseiny[2,3,*], A. M. Abdel-Gaber[1], M. E. Mohamed[1]

[1]Faculty of Science, Chemistry Department, Alexandria University, Alexandria, Egypt
[2]Faculty of Sciences, Chemistry Department, Jouf University, Jouf, Saudi Arabia
[3]Faculty of Science, Chemistry Department, Kuwait University, Kuwait

Abstract The role of air in the dissolution process of aluminium in 1.0 M HCl solution at room temperature was studied using gasometry, linear polarization, potentiodynamic polarization and electrochemical impedance spectroscopy (EIS) techniques. The kinetics of oxidation of aluminium in the air at room temperature was investigated using the EDX technique. The results show that the growth of the oxide film obeys the logarithmic law in short exposure time and the parabolic law in long exposure. Effect of Cl^- ion concentration and exposure time of aluminium to air at room temperature on the corrosion rate and incubation period of aluminium in 1.0 M HCl solution was studied using gasometry. The results show that the incubation period decreases, and the corrosion rate increases with increasing the Cl^- ion concentration. However, with increasing the exposure time, the incubation period increases but the corrosion rate decreases. A mechanism of dissolution of aluminium in 1.0 M HCl solution was suggested and fitted to the experimental results.

Keywords Aluminium, Oxidation, Room temperature, EDX, Corrosion

1. Introduction

Aluminium and its alloys represent an important category of material due to their low density, pleasing appearance, and wide range of industrial applications, especially in aerospace and corrosion resistance. For these reasons, the electrochemical behaviour of aluminium and its alloys has attracted the attention of many investigators [1–6] aluminium has a strong chemical affinity to oxygen that makes it easy to produce an air-formed oxide film. The oxidation is initially extremely rapid, but after a few minutes or hours, it drops to very low or negligible values, a stable film being formed 20-100 °A thick [7]. Mott [8] explained this behaviour based on the hypothesis that a strong field is set up in the oxide film due to a contact potential difference between metal and adsorbed oxygen, which enables the metal ions to move through it without much support from temperature. The kinetics of the reaction is best described by a logarithmic growth law.

Aluminium oxide is chemically inactive and the passive behaviour of aluminium is based on this inactivity [9]. Lorking and Mayne [10,11] reported that, when the oxide film dissolves, the metal corrodes uniformly, and the corrosion is associated with the initial thickness of the oxide film. On the other hand, localized corrosion occurs when the film is damaged under conditions that prohibit normal self-repair [12]. The protection of aluminium against corrosion in aqueous media by the easily formed protective oxide layer is affected by the presence of Cl^- ions. This type of corrosion is used to a good advantage in the etching of aluminium in strong hydrochloric acid solution for use in dielectric capacitors [13]. It is well known that Cl^- ion is important in determining the corrosion rate. A work using radioactive labelled Cl^- ions has shown that chloride does not enter into the oxide film but is chemisorbed onto the oxide surface and acts as a reaction partner, aiding dissolution via the formation of oxychloride complexes [14].

Several mechanisms for the dissolution of aluminium in an acid solution containing Cl^- ions have been reported in the literatures. Foly [15] proposed a mechanism stating that, aluminium reacts with water and H^+ ions through three steps producing $[AlOH]^{2+}$ cation, which reacts with Cl^- ions giving $[AlOHCl]^+$ through the fourth step. In previous work [16], it was proposed that Cl^- ions are adsorbed on the aluminium surface in competition with chemisorbed oxygen molecules from dissolved oxygen, followed by a slow dissolution step which catalyzed by Cl^- ions. Recently, another mechanism was suggested [17] and stated that molecular oxygen gas is firstly chemisorbed on the aluminium surface followed by

* Corresponding author:
Sherifelhousseiny2040@gmail.com (S. El-Housseiny)
Received: May 27, 2022; Accepted: Jun. 13, 2022; Published: Jun. 24, 2022
Published online at http://journal.sapub.org/pc

Cl^- ion adsorption and formation of oxide-chloride complex in a slow step. In the presence of H^+ ions, the oxide-chloride complex exhibits fast dissolution.

This work aims to study the protective action of air in the dissolution of aluminium in 1.0 M HCl solution at room temperature. The dependence of the corrosion rate of aluminium on the exposure time in the air at room temperature was investigated using gasometry, potentiodynamic polarization and electrochemical impedance spectroscopy (EIS) techniques. The kinetics of oxidation of aluminium in the air at room temperature was studied using EDX. Effect of Cl^- ion concentration at different exposure times on the rate of dissolution of aluminium in 1.0 M HCl solution was studied and a mechanism of dissolution of aluminium was suggested.

2. Experimental

2.1. Gasometry Measurements

Aluminium sheet samples having area of $1cm^2$ were placed in Mylius vessel containing 1.0 M HCl solition. The Mylius vessel allows measuring the volume of evolved hydrogen gas as a function of time [16].

2.2. Electrochemical Measurements

Electrochemical impedance, **linear and potentiodynamic polarization measurements** were carried out using a frequency response analyzer potentiostat (PARSTAT, USA). The frequency range studied was $0.1 \leq f \leq 1.0 \times 10^4$ Hz. with applied potential signal amplitude of 10 mV around the rest potential. A three electrode mode cell contains a saturated calomel reference electrode and an auxiliary graphite electrode was used. The working aluminium electrode was fabricated in a cylindrical form and encapsulated in epoxy resin in such a way that only one surface was left uncovered and thus avoids crevice effect. A long screw fastened to one end of the test cylinder for electrical connection. The Teflon gasket thereby forms water tight seal with the specimen electrode that prevents migration of any electrolyte. The elemental composition of the working electrode is: (% wt) 99.687% Al, 0.001% Mn, 0.001% Ni, 0.001% Zn, 0.003% Ti, 0.171% Fe, 0.135% Si, 0.001% Cu. The exposed area of the working electrode was polished using different grade emery paper 320, 600, 1000 and 1200 grit starting with a coarse one and proceeding in steps to the fine grit up to a mirror finish, washed thoroughly with double distilled water and finally dried by absolute ethanol. The working electrode was introduced into the test solution and left 20 minutes to attain the open circuit potential before polarization and EIS measurements. The polarization curves were recorded at a scan rate of 20 mV/min. started from cathodic potential (E_{rest} - 300 mV) going to the anodic direction. The values of linear polarization resistance were estimated from the slope of potential-current curve within ± 20 mV around the open circuit potential. All the experiments were done at 30℃ in a solution open to the atmosphere under unstirred conditions. To test the reliability and reproducibility of the measurements, duplicate experiments were performed in each case of the same conditions.

2.3. Scanning Electron Microscope (SEM) and Energy Dispersive X-ray Spectrometer (EDX)

The morphology of the aluminium coupons was investigated by SEM using a JEOL JSM-700F Field Emission SEM instrument. The elemental composition of the aluminium surface was analyzed by energy dispersive x-ray spectrometer (EDS, JEM-2100, Japan).

2.4. Preparation of Solutions

Stock solutions of 5M HCl and 5M NaCl were prepared from HCl and NaCl, obtained from SIGMA-ALDRICH. To prepare 1.0 M HCl solution, 5 mL of 5M HCl solution was placed in 50 mL measuring flask and completed to the mark with distilled water. However, in the case of 1.0 M HCl solution containing different concentrations of NaCl, 5 mL of 5 M HCl and the required volume of 5 M NaCl were placed in 50 mL measuring flask and completed to the mark with distilled water.

3. Results and Discussion

3.1. Effect of Exposure Time of Aluminium in Air at Room Temperature on Its Corrosion Rate

To investigate the protective action of the air formed oxide film on aluminium at room temperature, several polished aluminium samples were exposed to air for different periods. Then the rate of dissolution of aluminum samples in 1.0 M HCl solution was examined by gasometry, potentiodynamic polarization, and electrochemical impedance spectroscopy techniques.

Figure 1 shows that the evolution of hydrogen gas commences only after a certain time from the immersion of the aluminium in 1.0 M HCl known as the incubation (or inductive) period. This time may correspond to the period required to destroy the pre-immersion formed oxide film. The shorter induction time appeared for freshly polished aluminium, where there are no oxide films, corresponds to the time required to overcome the slow discharge or recombination step for the hydrogen evolution and saturation of the acid solution by the evolved gas. After the incubation period, the volume of hydrogen gas evolved varies linearly with immersion time. The rate of corrosion was assessed from the slope of a tangent to the rising part of the evolution curve. Moreover, the incubation period was determined from the intercept of the tangents with the x-axis.

Figure 2 shows a decrease of the corrosion rate, the rate of hydrogen gas evolution and an increase of the incubation period with the time of exposure to air. Since for hydrogen

gas to evolve, electrons should be transferred through the surface oxide on aluminium. This indicates that the electronic resistance of the oxide film can affect the corrosion rate of the oxide film [18]. By increasing the thickness of the natural oxide film, much better surface protection can be achieved [19]. Therefore, the decrease in corrosion rate may be attributed to the formation of thicker oxide film so its breakdown by the acid becomes harder [16].

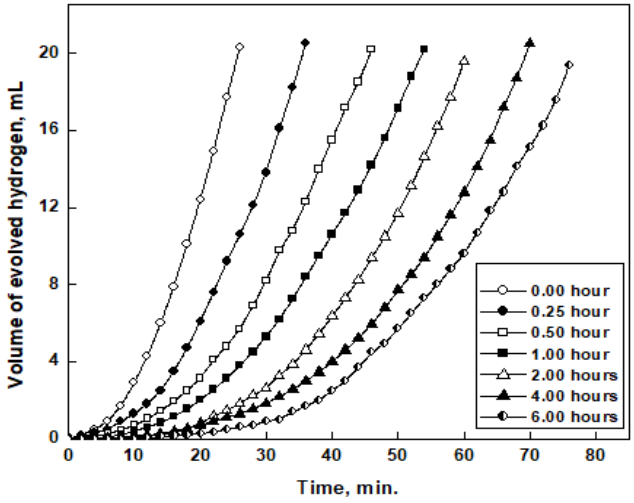

Figure 1. Variation of the volume of hydrogen gas evolved with time for aluminium immersed in 1.0 M HCl after exposure to air for different times

The potentiodynamic polarization curves of aluminium, exposed to air at room temperature to different periods in 1.0 M HCl solution, shown in Figure 3, indicate that the time of exposure to air affect predominantly the cathodic part of the polarization curves. It is well known that during metal corrosion, the rate of oxidation equals the rate of reduction in terms of electron production and consumption. This leads to the fact that inhibiting the hydrogen evolution reaction by the air-formed oxide film retards the metallic corrosion [18].

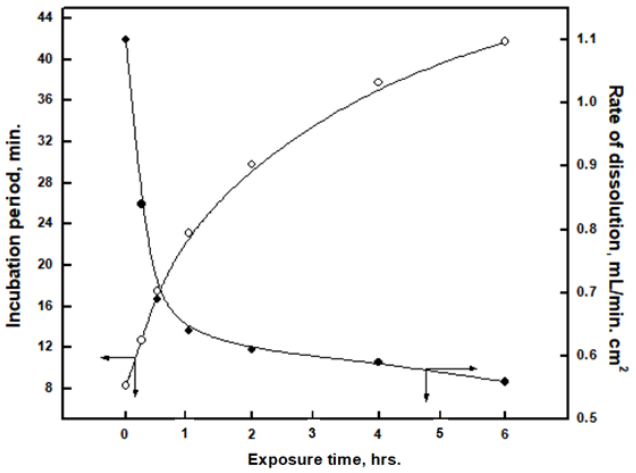

Figure 2. Variation of incubation period and corrosion rate with the exposure time of aluminium to air before immersion in 1.0 M HCl solution

Applying Tafel extrapolation method on the linear parts of anodic and cathodic polarization curves gives corrosion current density, i_{corr}. The decrease of corrosion current density with increasing the exposure time to air, Figure 4, is mainly attributed to the increase of the thickness and decrease in the porosity of the oxide film. Table 1 shows the corrosion potential and the anodic and cathodic Tafel slopes, β_a and β_c, respectively, of aluminium exposed to air at room temperature to different periods in 1.0 M HCl solution. The results show that increasing the exposure time has a small effect on both corrosion potential and Tafel slopes of aluminium in 1.0 M HCl solution.

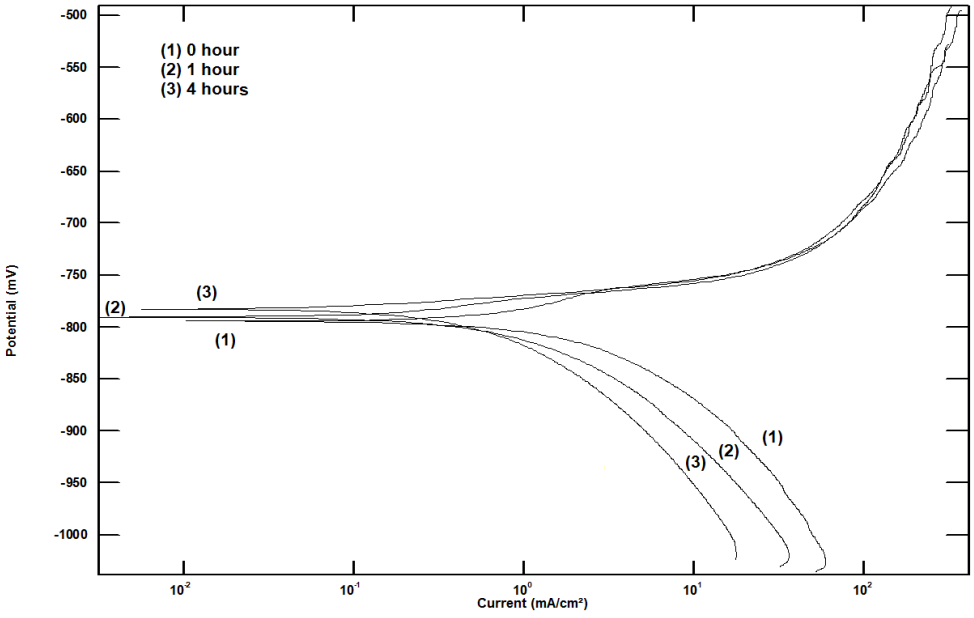

Figure 3. Potentiodynamic polarization curves for aluminum in 1.0 M HCl solution after different exposure times to air at room temperature

Table 1. The corrosion potential, and the anodic and cathodic Tafel slopes, β_a and β_c respectively, of aluminium in 1.0 M HCl solution after exposure to air at different periods at room temperature

Exposure time	-Ecorr (mV)	Ba mV/decade	Bc mV/decade
0.0	794	113	178
1.0	791	109	176
4.0	786	108	175

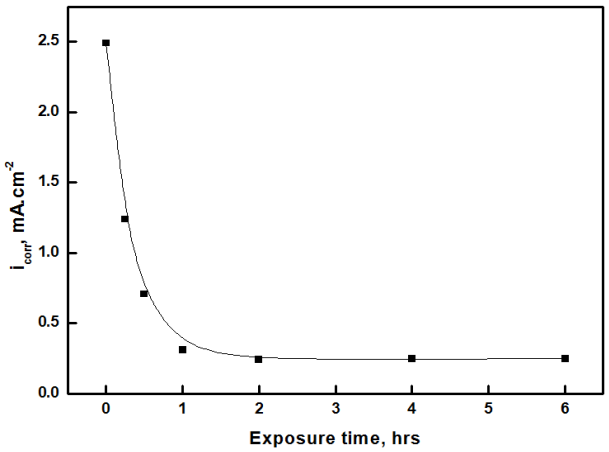

Figure 4. Variation of corrosion current density of aluminium in 1.0 M HCl solution after different exposure times to air at room temperature

The porosity of oxide films was estimated from polarization resistance measurements using the equation [20,21]:

$$\% \text{ Porosity} = [(R_{fp} / R_{ae}) 10\text{-}(\Delta E_{corr} / \beta a)] \text{ x}100$$

Where R_{fp} and R_{ae} are the polarization resistances of the freshly polished bare and air-exposed aluminium samples in 1.0 M HCl, respectively. ΔE_{corr} is the difference between the corrosion potentials of these samples. βa is referred to the slope of the anodic Tafel line derived from the polarization curves. The variation of porosity of the aluminium oxide with the exposure time is shown in figure 5, which shows a sharp decrease in the porosity for the pre-immersed oxide film within the first hour from 71 to 42%. However, long exposure has a slight effect on the porosity, from 42 to 30%.

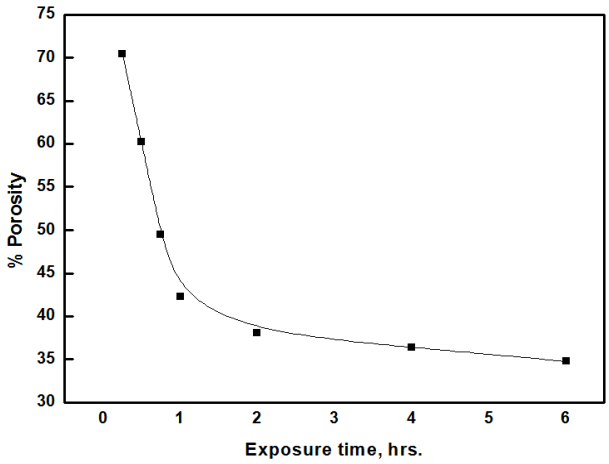

Figure 5. Variations of porosity of oxide film with exposure time

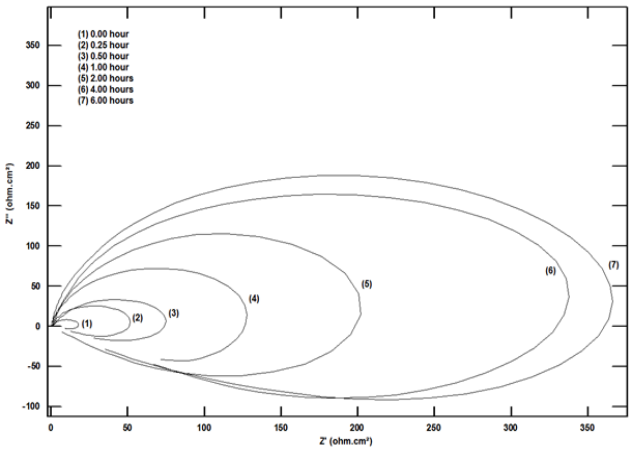

Figure 6. Nyquist diagrams for aluminium in 1.0 M HCl solution after exposure to air for different times at room temperature

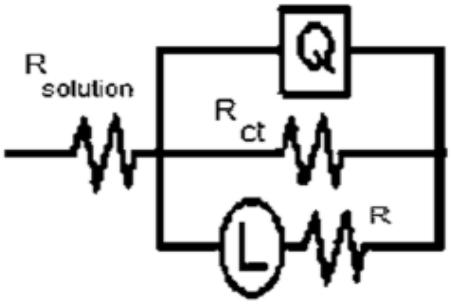

Figure 7. The equivalent circuit model

Figure 6 shows the Nyquist diagrams of dissolution of aluminium in 1.0 M HCl solution after exposure to air for different times at room temperature. The Nyquist plots were analyzed using the equivalent circuit shown in Figure 7 using the Zsimpwin program. The components of this circuit are the solution resistance, R_{sol}.; constant phase element, CPE; charge transfer resistance, R_{ct}; an inductor (L) with a polarization resistance R_p. The Nyquist curves exhibit a capacitive loop at a high frequency above the real axis and an inductive loop at a low frequency below the real axis. The capacitive loop is related to the oxide film formed on the aluminium surface, and the inductive loop below the real axis is attributed to the slow relaxation of $O_{2\,(g)}$ adsorption process, oxide dissolution, and aluminium dissolution [22,23].

The size of the Nyquist plots semicircles increases with the exposure time, indicating that the thickness of the oxide film increases and the porosity decreases with the exposure time. The charge transfer resistance can be used as a measure for corrosion resistance of the metal, which consequently reflects the nature of the formed oxide film. Figure 8 shows the increase of the charge transfer resistance and decrease of non-ideal double-layer capacitance for aluminium with the time of exposure to air. The decrease in Q_{dl} is an indication of oxygen adsorption or increasing film thickness over the metal surface.

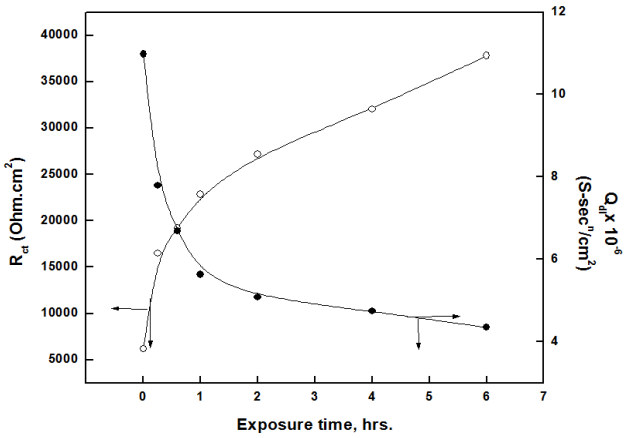

Figure 8. Variation of charge transfer resistance and none ideal double-layer capacitance of aluminium in 1.0 M HCl with the time of exposure to air

3.2. Kinetics of Oxidation of Aluminium in Air at Room Temperature

Figures 9 (a-f) represent the SEM micrographs and the corresponding EDX analysis of aluminium just polished and after exposure to air for 1 and 6 hours at room temperature. It is clear that the SEM micrograph (a) of just polished aluminium shows clear visible polishing marks on the surface and the EDX micrograph, Figure 9b, does not display the characteristic oxygen peak indicating that there is no adsorption of oxygen gas or formation of oxide film on the aluminium surface. Exposure of aluminium to air for 1 and 6 hours (micrographs c and e) leads to the disappearance of the polishing marks and the formation of a complete film of aluminium oxide. EDX analysis, figures 9 (d and f) show a corresponding increase of wt% O from 0.015 for aluminium exposed to air for 1 hour and 0.038 for a sample exposed to air at room temperature for 6.00 hours.

Figure 10 shows the variation of the oxygen uptake (wt% O) with the exposure time. Fitting the experimental data to the kinetic laws of oxidation are presented in figures 11 (a and b) show that the logarithmic law is fitted in a short exposure period, less than 1 hour (rate constant, k_l= 0.018). However, the parabolic law was obeyed in a long exposure period (rate constant, kp = 2.40 x 10^{-4}). These results explain the data obtained from the different techniques for measuring the corrosion rate of aluminium exposed to air at room temperature for different periods, gasometery, figure 2, potentiodynamic polarization, figure 4, porosity, figure 5, and electrochemical impedance, fig 8. For an exposure period less than one hour, the oxide film formed is thin and porous and its growth is controlled by logarithmic law. However, the oxide film formed at a long exposure period is less porous and thicker, and its growth is controlled by parabolic law.

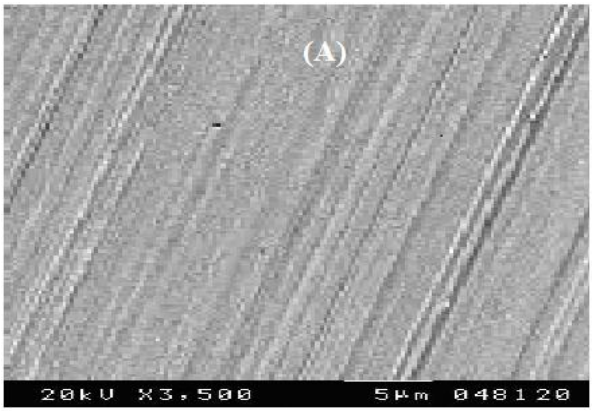

(a) Just polished

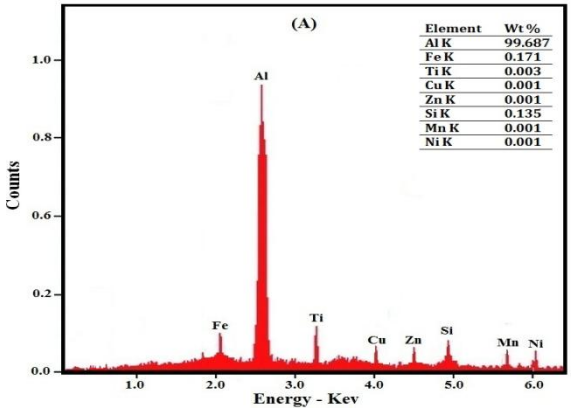

(b) Just polished

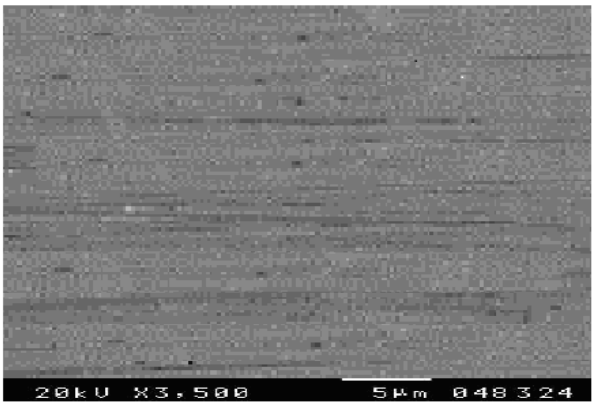

(c) 1.0 hour.

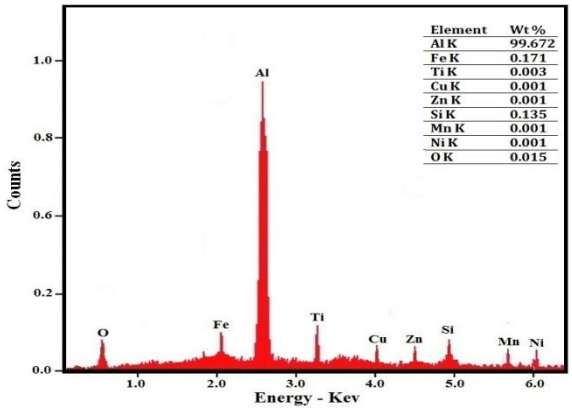

(d) 1.0 hour.

(e) 6.0 hours.

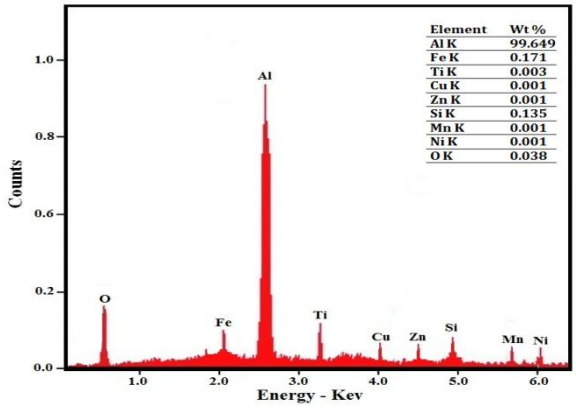

(f) 6.0 hours.

Figure 9(a-f). SEM and EDX micrographs, for (a, b) just polished aluminium and after exposure to air for (c,d) 1.0 hr and (e, f) 6.0 hours at room temperature

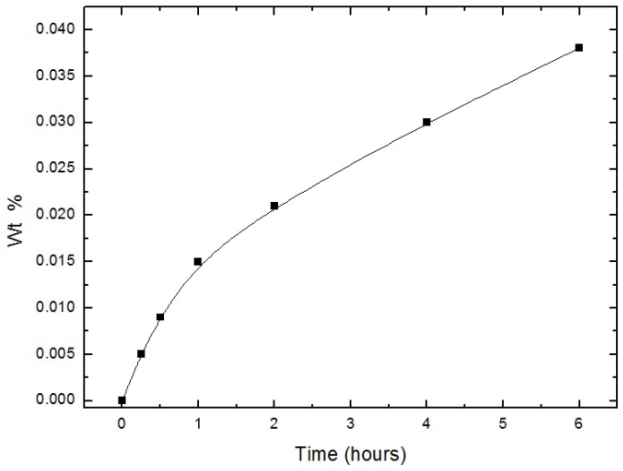

Figure 10. Variation of weight % of O_2 on the polished aluminium surface with time of exposure to air at room temperature

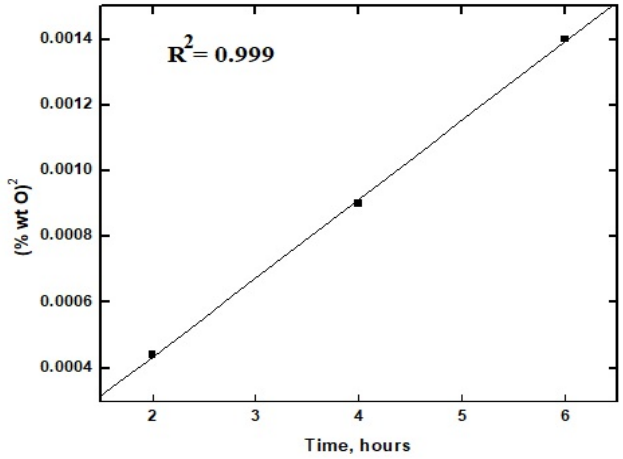

Figure 11b. Fitting the experimental data to parabolic law of the growth of aluminium oxide film at room temperature (long exposure, more than one hour)

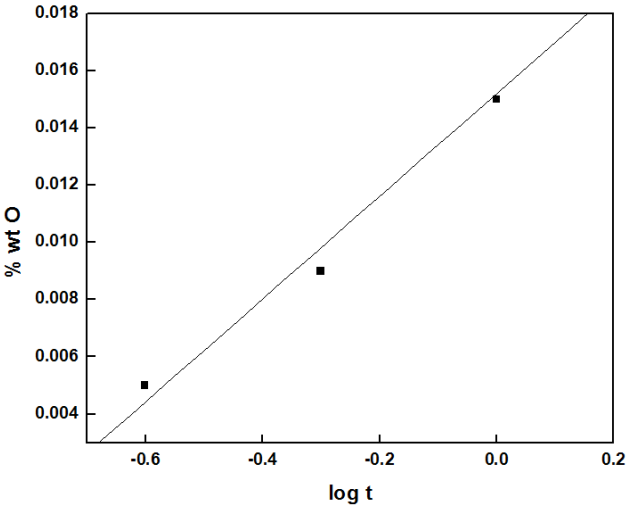

Figure 11a. Fitting the experimental data to the logarithmic law of the growth of aluminium oxide film at room temperature (short exposure, less than one hour)

3.3. Effect of Cl^- Ion Concentration on the Corrosion Rate of Al Exposed to Air at Room Temperature for Different Periods of Time- Mechanism of Corrosion of Al in 1.0M HCl

Figure 12 shows the variation of the volume of hydrogen gas evolved with time for aluminium exposed to air for 1 hour in 1.0 M HCl containing different chloride ions concentrations. The rate of dissolution of aluminium, represented by the slope of the straight part obtained after incubation period, increases with increasing chloride ion concentration. Similar measurements were made for Al exposed to air for 0.25hr (not shown).

Figures 13(a, b) show the effect of chloride ion concentrations on the incubation period and rate of dissolution of aluminium that was exposed to air for 0.25 and 1.0 hr., in 1.0M HCl containing different concentrations of Cl^- ion.

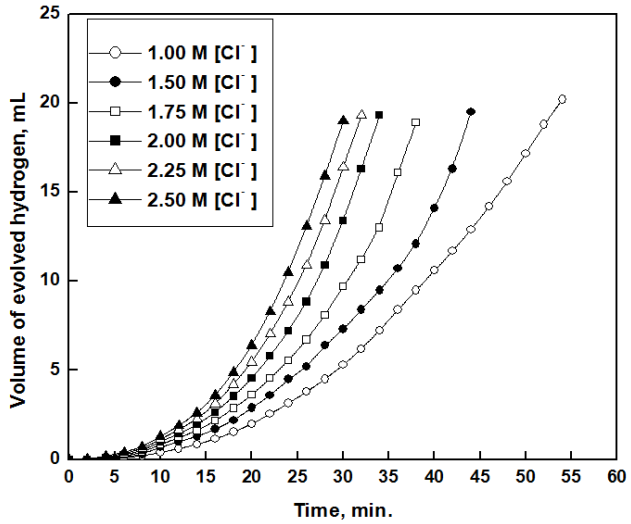

Figure 12. Variation of the volume of hydrogen gas evolved with time for aluminium in 1.0M HCl containing different chloride ions concentrations after exposure to air for one hour

The results indicate that the incubation period decreases with increasing Cl^- ion concentration but the rate of dissolution increases exponentially. The figure also shows that the rate of dissolution of aluminium in solutions containing the same concentration of chloride ion decreases with increasing the exposure time. This behavior can be discussed on the following basis: in the case of complete dissolution of oxide film that formed during the exposure period, the rate of dissolution of metal will be the same for Al samples exposed to air for different periods. However, this is not the case in the current study, where the dissolution rate of aluminium depends and decreases with increasing the exposure time. This indicates that the surface of the aluminium metal is still covered with partial oxide film during the dissolution of the metal after the incubation period. This argument can be confirmed by the following scanning and EDX analysis.

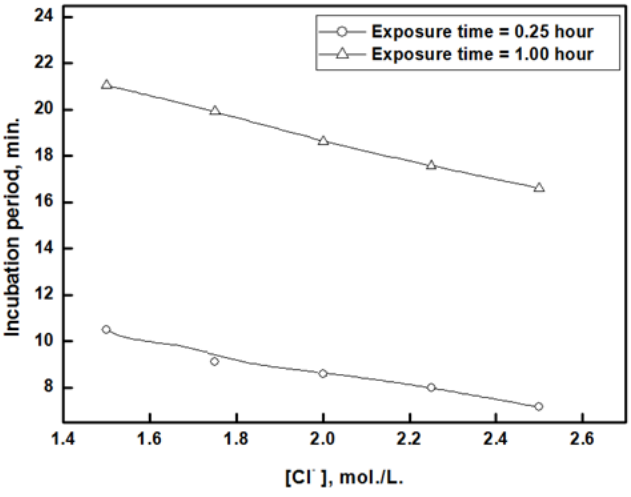

Figure 13(a). Variation of the incubation period with chloride ions concentration for aluminium in 1.0M HCl containing different chloride ions concentrations

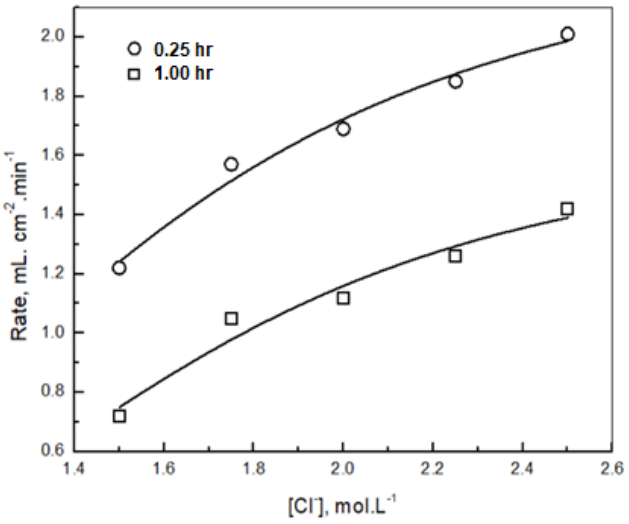

Figure 13(b). Variation of the rate of dissolution of aluminium in 1.0M HCl containing different chloride ions concentrations, exposed to air for 0.25 hr and 1.0 hr with chloride ions concentration and its non-linear curve fit

Figures 14(a and c) shows the morphology of the remaining oxide film of the air-exposed aluminium surface after 0.50 hour of immersion in 1.0 M HCl. Figure 14a shows that, for the oxide film formed after 0.25 hour of air exposure, some parts of the oxide film still adhere to the surface, and some parts crack. On the other hand, the oxide film remains intact on the surface after 1.00 hour of air exposure, Figure 14c. Figures 14(b and d) indicate that the wt% O obtained from EDX analysis increases with the time of exposure to air, from 0.003 to 0.007 for 0.25 and one hour exposure, respectively.

The obtained data suggested a dissolution mechanism consists of a series of the following steps: the first one is the adsorption of x moles of chloride ions over Al_2O_3 surface forming $Al_2O_3 : x\,Cl^-_{ads}$, the second step is slow and represents the formation of the aluminium oxo-chloro complex $[Al_2O_3Cl_x]^{-x}$, and the last one includes a fast reaction between the complex and the hydrogen ions in the solution giving aluminium cation and chloride ions.

$$Al_2O_3 + x\,Cl^- \underset{}{\overset{K}{\rightleftharpoons}} Al_2O_3 : x\,Cl^-_{ads}$$

$$Al_2O_3 : xCl^-_{ads} \xrightarrow{k} [Al_2O_3\,Cl_x\,]^{x-}$$

$$[Al_2O_3\,Cl_x\,]^{x-} + 6H^+ \xrightarrow{fast} 2Al^{3*} + 3H_2O + x\,Cl^-$$

This mechanism was used to derive the kinetic equation

$$Rate\ (V) = k\,[Al_2O_3 : x\,Cl^-_{ads}] \quad (1)$$

$$K = \frac{[Al_2O_3 : x\,Cl^-_{ads}]}{[Al_2O_3]\,[Cl^-]^x} \quad (2)$$

From equation (2)

$$[Al_2O_3 : x\,Cl^-_{ads}] = K\,[Al_2O_3]\,[Cl^-]^x \quad (3)$$

From equations (1) and (3)

$$Rate\ (V) = k\ K\,[Al_2O_3]\,[Cl^-]^x \quad (4)$$

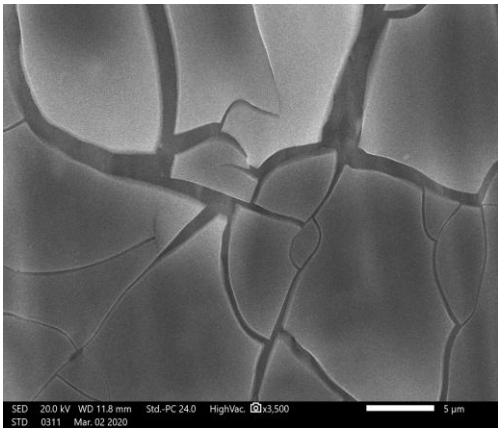

a) 0.25 hr.

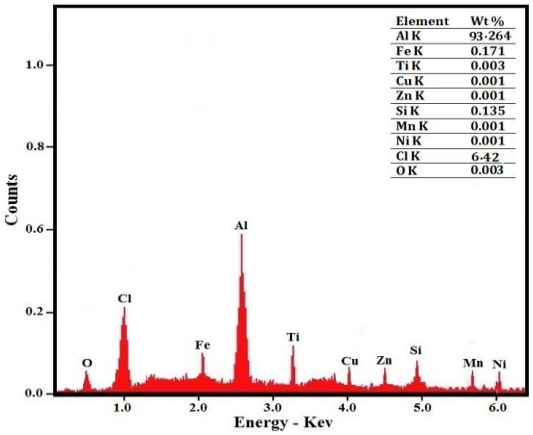

b) 0.25 hr.

c) 1.0 hr.

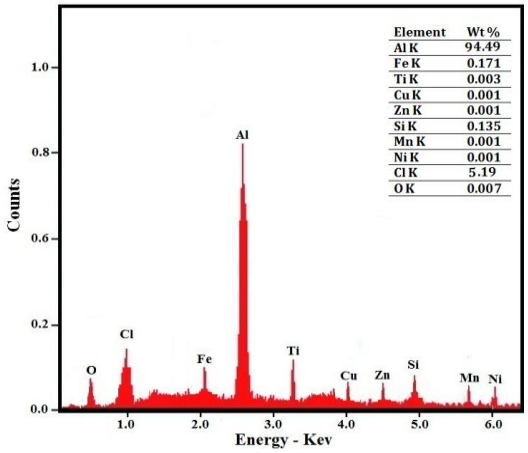

d) 1.0 hr.

Figure 14(a-d). SEM and EDX micrographs for aluminium immersed in 1 M HCl for 0.5 hour after exposure to air for (a, b) 0.25 hour and (c, d) 1.0 hour at room temperature

Since,

$$\sum \text{Al} = [Al_2O_3] + [Al_2O_3 : x\, Cl^-_{ads}] \quad (5)$$

From equations (3) and (5)

$$\sum \text{Al} = [Al_2O_3] + K\,[Al_2O_3]\,[Cl^-]^x \quad (6)$$

$$\sum \text{Al} = [Al_2O_3]\,(1 + K\,[Cl^-]^x) \quad (7)$$

$$[Al_2O_3] = \frac{\sum \text{Al}}{(1 + K\,[Cl^-]^x)} \quad (8)$$

Substitute into equation (4)

$$\text{Rate (V)} = \frac{k\,K \sum \text{Al}\,[Cl^-]^x}{(1 + K\,[Cl^-]^x)} \quad (9)$$

$$\text{Rate (V)} = \frac{k_{obs}\,[Cl^-]^x}{(1 + K\,[Cl^-]^x)} \quad (10)$$

In order to fit the validity of the proposed kinetic equation, a non-linear curve fit of the derived kinetic equation to the obtained experimental data, shown in figure 13b, was carried out. The obtained kinetic parameters were calculated and presented in Table 2. The data indicated that the number of moles of chloride ions adsorbed is nearly ≈3. Moreover, the observed rate constant, k and the equilibrium constant, K, decrease with increasing the exposure time. This behavior can be discussed on the basis that for long exposure, there is an increase of the thickness and decrease of the porosity of Al_2O_3 film, leading to the decrease of the diffusion path, which retard the penetration of chloride ions to attack the metal at the interface between the oxide and the metal.

Table 2. Kinetic parameters for aluminium in 1.0M HCl after exposure to air for a different period

Exposure time, min	k_{obs}	K	x
0.25	0.735	0.314	3.16
1.0	0.317	0.191	3.61

4. Conclusions

Gasometry, potentiodynamic polarization and electrochemical impedance spectroscopy results indicated that the exposure of aluminium metal to air at room temperature leads to an increase of the incubation period and a decrease of the corrosion rate of the metal in 1.0 M HCl solution. EDX analysis for freshly polished aluminium surface indicated that there is no adsorption of oxygen and hence no formation of the oxide layer. The growth of the oxide film obeys the logarithmic law in short exposure time,

less than one hour, and the parabolic law in long exposure, up to six hours.

Effect of the Cl^- ion concentration on the incubation period and corrosion rate of aluminium in 1.0 M HCl containing different concentrations of Cl- ions was investigated using the gasometry technique; the results indicated that the incubation period decreased with increasing the Cl^- ion concentration, however the corrosion rate decrease. Also, in the presence of the same Cl^- ion concentration, the corrosion rate decrease with increasing the exposure time, indicating that the oxide film still partially covers the aluminium surface during corrosion after the incubation period, the EDX results confirmed this argument.

A mechanism of dissolution of aluminium was proposed, which contains three steps: the first one is the adsorption of "x" moles of Cl^- ions over Al_2O_3 surface, the second step is a slow formation of the oxo-chloro complex, and the last one is the fast dissolution of the complex in the acid solution. The kinetic parameters obtained from the non-linear curve fit of the derived equation after 0.25 and 1.0 h exposure periods confirmed the obtained results.

Declarations

Contributions

All authors conceived the presented idea. El-Housseiny, S. & Mohamed, M. E. were responsible for the experimental work. Abd-El-Nabey, B. A., Mohamed, M. E. & Abdel‑Gaber , A. M. was responsible for the discussion of data. All authors contributed to the final manuscript.

Competing interests

The authors declare no competing interests.

Data availability

All the data presented in the current study are available from the corresponding author on reasonable request.

Funding

This research did not receive any specific grant from funding agencies in the public, commercial, or not-for-profit sectors.

REFERENCES

[1] J.W. Diggle, T.C. Downie, C.W. Goulding, The dissolution of porous oxide films on aluminium, Electrochim. Acta. 15 (1970) 1079–1093. https://doi.org/10.1016/0013-4686(70)85002-2.

[2] B.W. Samuels, K. Sotoudeh, R.T. Foley, Inhibition and Acceleration of Aluminum Corrosion, Corrosion. 37 (1981) 92–97. https://doi.org/10.5006/1.3593852.

[3] M. Baumgärtner, H. Kaesche, Aluminum pitting in chloride solutions: morphology and pit growth kinetics, Corros. Sci. 31 (1990) 231–236.

[4] C.M.A. Brett, On the electrochemical behaviour of aluminium in acidic chloride solution, Corros. Sci. 33 (1992) 203–210. https://doi.org/10.1016/0010-938X(92)90145-S.

[5] L. Garrigues, N. Pebere, F. Dabosi, An investigation of the corrosion inhibition of pure aluminum in neutral and acidic chloride solutions, Electrochim. Acta. 41 (1996) 1209–1215. https://doi.org/10.1016/0013-4686(95)00472-6.

[6] S.E. Frers, M.M. Stefenel, C. Mayer, T. Chierchie, AC-Impedance measurements on aluminium in chloride containing solutions and below the pitting potential, J. Appl. Electrochem. 20 (1990) 996–999. https://doi.org/10.1007/BF01019578.

[7] H. Friedenstein, S.L. Martin, G.L. Munday, G. Dearnaley, A.M. Stoneham, D. V Morgan, W.F. Berg, J.A. Ramsey, J. Garlick, J.K. Roberts, N. Cabrera, N.F. Mott, Theory of the oxidation of metals The mechanism of the thermionic emission from oxide coated cathodes The growth and structure of semiconducting thin films B A Joyce Electrical phenomena in amorphous oxide films Latent image formation in photographic silv, Rep. Prog. Phys. 12 (1949). http://iopscience.iop.org/0034-4885/12/1/308.

[8] N.F. Mott, The theory of the formation of protective oxide films on metals., Trans. Faraday Soc. 43 (1946) 429–434.

[9] H.P. Godard, W.P. Jepson, M.R. Bothwell, R.L. Kane, The Corrosion of Light Metals, New York, Wiley, 1967.

[10] K.F. Lorking, J.E.O. Mayne, The corrosion of aluminium, J. Appl. Chem. 11 (2007) 170–180. https://doi.org/10.1002/jctb.5010110503.

[11] K.F. Lorking, J.E.O. Mayne, The corrosion of aluminium in solutions of sodium fluoride and sodium chloride, Br. Corros. J. 1 (1966) 181–182. https://doi.org/10.1179/000705966798327795.

[12] C. Edeleanu, U.R. Evans, The causes of the localized character of corrosion on aluminium, Trans. Faraday Soc. 47 (1951) 1121–1135. https://doi.org/10.1039/tf9514701121.

[13] W.M. Moore, C.-T. Chen, G. A. Shirn, A voltammetric investigation of AC corrosion phenomena at an aluminum electrode in hydrochloric acid, Corros. 40 (1984) 644–649.

[14] L. Tomcsányi, K. Varga, I. Bartik, H. Horányi, E. Maleczki, Electrochemical study of the pitting corrosion of aluminium and its alloys—II. Study of the interaction of chloride ions with a passive film on aluminium and initiation of pitting corrosion, Electrochim. Acta. 34 (1989) 855–859.

[15] T.H. Nguyen, R.T. Foley, The Chemical Nature of Aluminum Corrosion: II. The Initial Dissolution Step, J. Electrochem. Soc. 129 (1982) 27–32. https://doi.org/10.1149/1.2123768.

[16] A.A. El-Awady, B.A. Abd-El-Nabey, S.G. Aziz, Thermodynamic and kinetic factors in chloride ion pitting and nitrogen donor ligand inhibition of aluminium metal corrosion in aggressive acid media, J. Chem. Soc. Faraday Trans. 89 (1993) 795–802. https://doi.org/10.1039/FT9938900795.

[17] A.M. Abdel-Gaber, B.A. Abd-El-Nabey, I.M. Sidahmed, A.M. El-Zayady, M. Saadawy, Kinetics and thermodynamics of aluminium dissolution in 1.0 M sulphuric acid containing chloride ions, Mater. Chem. Phys. 98 (2006) 291–297.

[18] E.J. Lee, S.I. Pyun, The effect of oxide chemistry on the passivity of aluminium surfaces, Corros. Sci. 37 (1995) 157–168. https://doi.org/10.1016/0010-938X(94)00127-R.

[19] G. Hass, On the Preparation of Hard Oxide Films with Precisely Controlled Thickness on Evaporated Aluminum Mirrors, J. Opt. Soc. Am. 39 (1949) 532–540.

[20] H.Y. Su, C.S. Lin, Effect of additives on the properties of phosphate conversion coating on electrogalvanized steel sheet, Corros. Sci. 83 (2014) 137–146. https://doi.org/10.1016/j.corsci.2014.02.002.

[21] B.A. Abd-El-Nabey, S. El-Housseiny, H.M. El-Kshlan, M.A. Abd-El-Fatah, Effect of Surfactants on the Protection Efficiency of Zn-Phosphate Coat on Steel, 7 (2017) 75–86. https://doi.org/10.5923/j.pc.20170704.01.

[22] X. Li, S. Deng, X. Xie, Experimental and theoretical study on corrosion inhibition of oxime compounds for aluminium in HCl solution, Corros. Sci. 81 (2014) 162–175. https://doi.org/10.1016/j.corsci.2013.12.021.

[23] H.A. - Fetouh, B.. Abd-El-Nabey, Y.M. , Goher, M.S. Karam, Electrochemical Investigation of the Anticorrosive Properties of Silver Nanoparticles for the Acidic Corrosion of Aluminium, J. Electrochem. (2018) 89–100.